OPTIMAL DESIGN OF GUIDE VANE IN THE CYCLONE VORTEX FINDER BASED ON ORTHOGONAL ANALYSIS

Zhong HUANG[1 3], Ming LIU[2], Guanjie LIU[3], Fengyang WANG[3], Defu CHE[1 *]

[1]*The State Key Laboratory of Multiphase Flow in Power Engineering, Xi'an Jiaotong University, Xi'an, 710049, China*

[2]*State Key Laboratory of Hydroscience and Engineering, Tsinghua University, Beijing, 100084, China*

[3]*China Huaneng Clean Energy Research Institute, Beijing, 102209, China*

*Email: chinacfb@gmail.com

Abstract – A new structure of installing guide vane inside eccentric vortex finder of cyclone was proposed. Five parameters including eccentric ratio e, blade number Z, hub inlet installing angle β, middle coefficient of hub installing angle k, shroud inlet installing angle increment Δβ were selected to design an orthogonal table of five elements and four levels. Based on RNG k-ε model, separation efficiencies of the conventional cyclone and 16 cyclones installing guide vanes inside vortex finder were calculated. By means of orthogonal analysis, the influence of each element has been ranked, and the optimal level of each element has been combined as the optimal structure. The simulation result indicated that the separation efficiency of the optimal structure has increased up to 7.04% while the pressure drop decreased no more than 12.5%. The flow field analysis showed the velocity in the inner vortex of cyclone was lower, while it was higher in the outer vortex, which is of great help for particle separation.

INTRODUCTION

Cyclone is a common equipment in industries, which can separate solid particles from gases under the effect of centrifugal force. Because of its simple structure, no moving parts, high separation efficiency and moderate pressure drop, cyclone is widely used for the flue gas with high temperature, high pressure and high dust content. It plays an important role in catalytic cracking, power generation and manufacturing, gas turbine and other fields.

Based on its operation principles, many researchers have come up with a variety of performance optimization methods. The aims of performance optimization usually focus on two aspects: 1) improving separation efficiency; 2) reducing pressure drop. Since the performance of conventional cyclone is limited by some drawbacks in structure design, progress has been made for structure optimization.

S. Bernardo (2005) found inlet section angle has a remarkable influence on cyclone performance. His numerical calculation results showed separation efficiency will reach the peak when inlet section angle is 45°. Further study was carried on by (Qian, 2009. Qian, 2007). It was found tangential velocity in inner vortex will decrease when inlet section angle increases, whereas tangential velocity in outer vortex will increase. Raoufi (2008) and Zenz (1993) investigated the influence of vortex finder diameter. Their research indicated that only proper size can lead to high separation efficiency. It is of great help to restrain the reentrainment at the solid outlet. Kirch (1982) proposed an approach of equipping anti-reentrainment cone. Hoffmann (1995) advised adding a long and straight tube outside the solid outlet.

The flow field in the cyclone is a complicated three-dimensional, two-phase flow pattern with turbulence and violent vortex. It is too complex to propose a mathematical model which can describe the flow mechanism in cyclone precisely. Most researches adopted the method of experiment or numerical simulation. In addition, with the rapid development of computer technology, computational fluid dynamics plays a more and more significant role in cyclone research due to its high efficiency and low cost. Numerical simulation based on Reynolds Stress Model (RSM) or Large Eddy Simulation (LES) has made a great progress on structure optimization of cyclone in recent years.

In this context, a new approach of structure design is proposed. Guide vanes are installed inside the vortex finder, as Fig.1. The shroud of guide vane is installed inside the vortex finder while the hub of guide vane is installed outside an inner tube in the vortex finder. The inlet of inner tube is made into a cone fairing, which

can guide the gas to flow into the vane. The entire vortex finder is eccentric installed against the inlet direction.

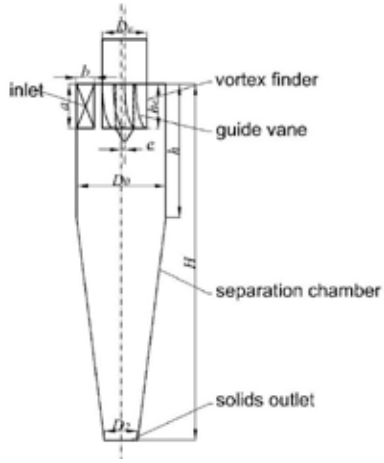

Fig.1. Cyclone with Guide Vane inside the Vortex Finder

1. Optimizing Scheme

1.1. Orthogonal Experiment Design

Orthogonal experiment design is a common method based on orthogonality, which consists of three parts: an orthogonal table, elements and levels. An orthogonal table should meet two rules. Firstly, different levels (line) of every element (column) appear with an equal number of times. Secondly, if the levels in the same line of any two elements are combined as an ordered pair, all possible ordered pair should appear once. For an experiment including m elements and r levels, it usually needs r^m experiments. However, it can be greatly reduced when the orthogonal experiment design is used.

1.2. Parameter Optimization

In this paper, five parameters are selected to optimize the structure of cyclone, which are eccentric ratio e, blade number Z, hub inlet installing angle β, middle coefficient of hub installing angle k, shroud inlet installing angle increment $\triangle\beta$. As a result of that, an orthogonal table of five elements and four levels is established as Table 1.

Table.1: Orthogonal Table

$L_{16}(4^5)$	e	Z	β	k	$\Delta\beta$	
1	0%	4	64	0.3	-15	E1Z1B1K1D1
2	0%	6	61	0.4	-18	E1Z2B2K2D2
3	0%	8	58	0.5	-21	E1Z3B3K3D3
4	0%	10	55	0.6	-24	E1Z4B4K4D4
5	2%	4	61	0.5	-24	E2Z1B2K3D4
6	2%	6	64	0.6	-21	E2Z2B1K4D3
7	2%	8	55	0.3	-18	E2Z3B4K1D2
8	2%	10	58	0.4	-15	E2Z4B3K2D1
9	4%	4	58	0.6	-18	E3Z1B3K4D2
10	4%	6	55	0.5	-15	E3Z2B4K3D1
11	4%	8	64	0.4	-24	E3Z3B1K2D4
12	4%	10	61	0.3	-21	E3Z4B2K1D3
13	6%	4	55	0.3	-21	E4Z1B4K2D3
14	6%	6	58	0.4	-24	E4Z2B3K1D4
15	6%	8	61	0.6	-15	E4Z3B2K4D1
16	6%	10	64	0.5	-18	E4Z4B1K3D2

2. Description of the Numerical Model

2.1. The Cyclone Model

In order to compare the efficiency of the optimal cyclone with that of the conventional cyclone, the geometry size of cyclone in this paper is totally the same as the one used in Hoffmann's experiment (1991). The diameter of the cyclone main body (D_0) is 200 mm, and the inlet velocity (v_0) is 15 m/s, as listed in Table 2.

Table. 2: Geometry Data of the Conventional Cyclone

a/D_0	b/D_0	D_e/D_0	h_e/D_0	h/D_0	H/D_0	D_2/D_0
0.5	0.2	0.5	0.5	1.5	4	0.35

2.2. Turbulent Model

Generally, the flow field in the cyclone is turbulent with violent vortex. The following RNG $k-\varepsilon$ Model is employed. The turbulent kinetic energy equation and the rate of dissipation equation is described by Eq. 1 and Eqs. 2:

$$\frac{\partial \rho k}{\partial t}+\frac{\partial\left(\rho U_j k\right)}{\partial x_j}=\frac{\partial}{\partial x_j}\left(\frac{\mu_{eff}}{\sigma_k}\frac{\partial k}{\partial x_j}\right)+G_k-\rho\varepsilon \tag{1}$$

$$\frac{\partial \rho \varepsilon}{\partial t}+\frac{\partial\left(\rho U_j k\right)}{\partial x_j}=\frac{\partial}{\partial t}\left(\frac{\mu_{eff}}{\sigma_\sigma}\frac{\partial \varepsilon}{\partial x_j}\right)+\frac{\varepsilon}{k}(C_{\varepsilon 1}G_k-C_{\varepsilon 2}\rho\varepsilon) \tag{2}$$

Note: Subscripts (j = 1, 2, 3) indicate the components in the Cartesian coordinate system;

ρ : density;

μ_{eff} : molecular viscosity;

G_k : turbulent kinetic energy volume production rates.

2.3. Boundary Conditions

In the numerical simulation, the boundary condition used at the cyclone inlet is a velocity-inlet boundary condition, and the inlet velocity (v_0) is 15 m/s. A pressure-outlet boundary condition is used at not only the gas outlet but also the solid outlet. The outlet pressure is 1 atm in every simulation. Noslip boundary condition is used at the wall boundary, and for the near-wall treatment, a scalable wall function is utilized. The simulation is solved in CFX 14.5.

2.4. Particle Distribution

In each simulation, the particle distribution is assumed to meet the Rosin-Rammler distribution as described by Eqs. 3.

$$Y_d=e^{-\left(d/\overline{d}\right)^n} \tag{3}$$

Note:

Y_d : the mass fraction of particles with a diameter larger than d ;

$\overline{d}$: meso-position diameter, 5 μm ;

n : dispersion index, 0.07.

3. Orthogonal Analysis

The orthogonal analysis is conducted as Table 3.

Table. 3: Orthogonal Analysis Table

	e	Z	β	k	$\Delta\beta$	Index η
1	1	1	1	1	1	91.353
2	1	2	2	2	2	92.892
3	1	3	3	3	3	93.249
4	1	4	4	4	4	92.285
5	2	1	2	3	4	92.453
6	2	2	1	4	3	93.348
7	2	3	4	1	2	93.124
8	2	4	3	2	1	92.985

9	3	1	3	4	2	92.859
10	3	2	4	3	1	93.280
11	3	3	1	2	4	93.444
12	3	4	2	1	3	92.682
13	4	1	4	2	3	91.991
14	4	2	3	1	4	92.215
15	4	3	2	4	1	92.123
16	4	4	1	3	2	92.000
K_1	369.779	368.656	370.145	369.373	369.741	
K_2	371.909	371.735	370.150	371.312	370.874	
K_3	372.265	371.940	371.307	370.982	371.270	
K_4	368.328	369.950	370.679	370.615	370.396	
R	0.984	0.821	0.291	0.485	0.382	

Note:
K_i: the sum of experiment results when level is i in the line;
R : range, $R = \max\{K_i\} - \min\{K_i\}$.

3.1. Primary and Secondary Analysis

Range reflects the influence of each element on the index. A large range represents a great impact, which likely indicates the element to be a primary element. Meanwhile, a small range represents a tiny impact, which is possible to be a secondary element. The degree of importance of the five elements can be ranked as Fig. 2 according to the range.

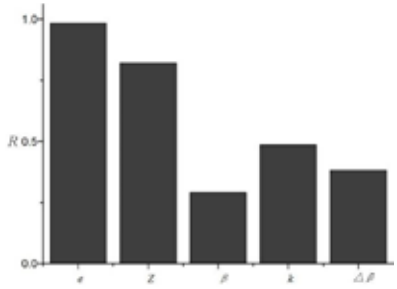

Fig.2. Range of Each Elements

Table. 4: Elements Rank

Index	Primary → Secondary				
Efficiency η	e	Z	k	$\Delta\beta$	β

3.2. Optimal Level

According to the K_i of each element, the optimal level can be selected by the biggest K_i.

As shown in Fig. 3, for all the five elements of eccentric ratio e, blade number Z, hub inlet installing angle β, middle coefficient of hub installing angle k, shroud inlet installing angle increment $\triangle\beta$, the index of efficiency increases first and then decreases with the level increasing. Each element should be selected at a proper level. A higher or lower level will lead to the decline of the efficiency.

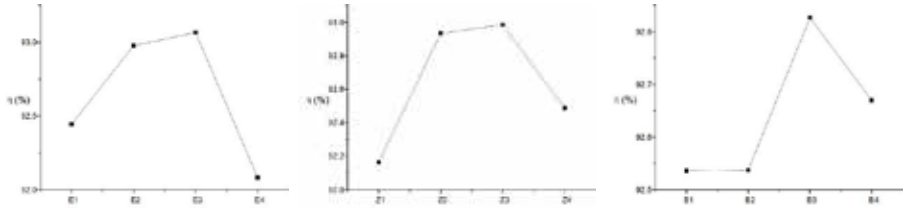

(a)eccentric ratio (b)blade number (c) hub inlet installing angle

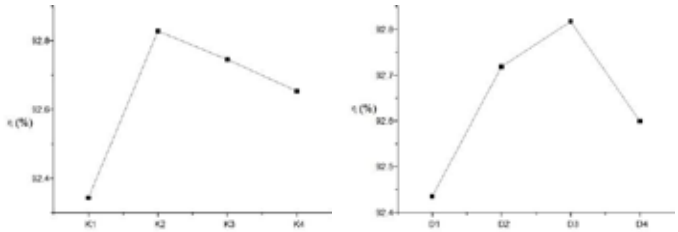

(d) middle coefficient of hub installing angle (e) shroud inlet installing angle increment

Fig.3. Relationship between each Element and Index

In this paper, a bigger index of efficiency will be more satisfying. As a result of that, the optimal level of each element can be selected according to Fig. 3. That is, E=E3，Z=Z3，B=B3，K=K2，D=D3. The exact data is as follows.

Table. 5: Optimal Level of Each Element

Index	Element				
	e	*Z*	*β*	*k*	*Δβ*
η	4%	8	58	0.4	-21

4. Flow Analysis

4.1. Separation Efficiency

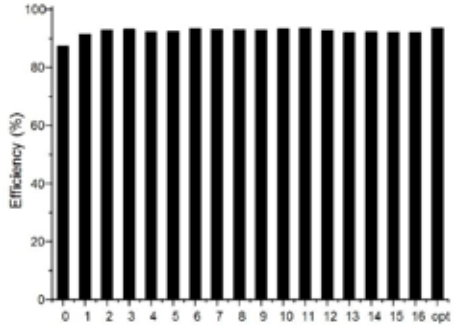

Fig.4. Separation efficiency

The separation efficiencies of all simulations are calculated as Fig. 4. The conventional cyclone without guide vane is shown as No. 0. The cyclones with guide vane inside the vortex finder according to Table. 1 are exhibited as No. 1 to No. 16, while the cyclone with optimal guide vane according to Orthogonal Analysis is presented as No. opt.

The simulation result of the conventional cyclone is 87.39%, and the result of experiment which Hoffmann (1991) has carried on with the cyclone of the same geometry size is 85%. The close efficiency of simulation and experiment proves the rationality of boundary conditions.

When guide vanes are installed inside the vortex finder, the separation efficiency has risen remarkably. Among the 16 orthogonal experiments, the separation efficiency rises by 4%-7%. It deserves to be mentioned that the cyclone with optimal guide vane has a separation efficiency of 93.543%, which increases by 7.04% compared with the simulation result of the conventional cyclone.

4.2. Pressure Drop

Though the separation efficiency can be improved by guide vanes, it is necessary to find out the influence upon the pressure drop. The pressure drop is calculated by CFX 14.5 in gas-phase separately with the same boundary conditions above. The simulation results are as Fig. 5.

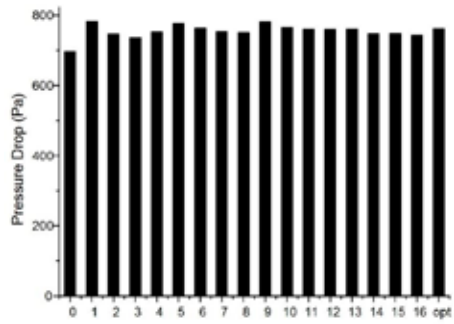

Fig. 5. Pressure Drop

After installing guide vanes inside the vortex finder, the pressure drop has risen by 5.77%-12.4%. In industrial applications, such growth can be accepted compared with the increase of the separation efficiency.

4.3. Flow Field

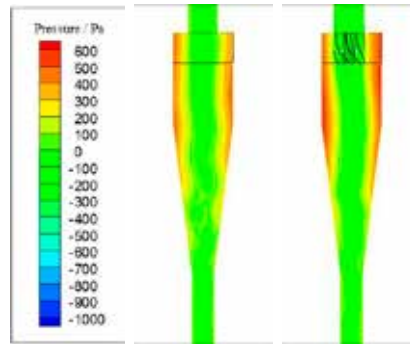

(a) Total Pressure

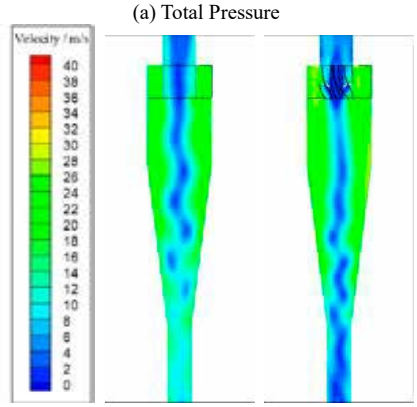

(b) Velocity

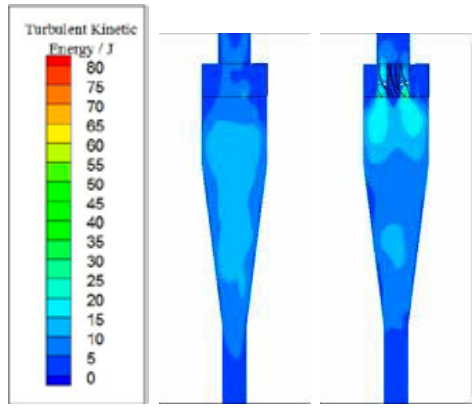

(e) Turbulent Kinetic Energy

Fig.6. Flow Field in the Cyclone

(Left: the conventional cyclone without guide vane; Right: the cyclone with optimal guide vane)

As shown in Fig. 6, the flow field in the cyclone has been improved after installing guide vanes inside the vortex finder. There are some obvious changes between these two kinds of cyclone as follows.

(1) The gas flow which undergoes a bottom-up movement in the center of cyclone, has converged to be a steady, upward main stream before entering the vortex finder.

(2) The inner vortex flow, which is formed from the area near solids outlet, has a smaller vortex radius. The gas velocity of inner vortex declines at the same time. As a result, the inner vortex becomes more concentrated.

(3) The concentration of inner vortex leads to the enhancement of outer vortex. The gas velocity rises near the imaginary cylinder surface, whose diameter is equal to the vortex finder.

(4) At the area near the inlet of guide vane, the turbulent kinetic energy is remarkably higher than other areas, which causes more pressure loss.

4.4. Velocity Distribution

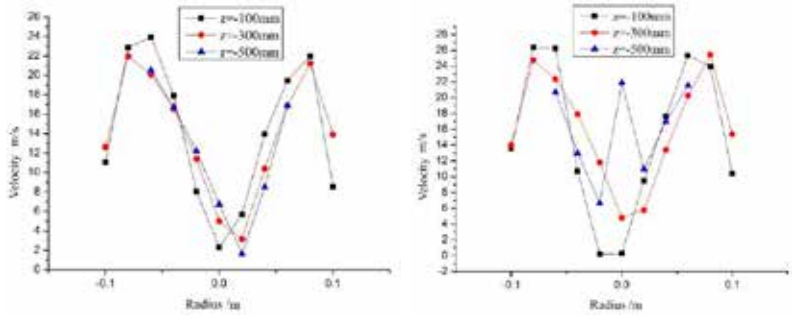

(a) the conventional cyclone without guide vane (b) the cyclone with optimal guide vane

Fig.7 Velocity Distribution in Different Cross Section

In Fig. 7, the cyclone ceiling surface is set as the cross section of z=0 mm, and the cross section z=-800 mm is solids outlet surface. Three cross sections have been selected to study the velocity distribution, including z=-100 mm, -300 mm and -500 mm.

As indicated by Fig. 7, the velocity distribution represents a shape of “M”. The velocity reaches the highest at the imaginary cylinder surface. The velocity of the inner vortex rises, and the velocity of the outer vortex decreases, when the height reduces. The velocity has a sharp decline near the wall because of viscosity effect.

Compared with the conventional cyclone, the velocity in the outer vortex of a cyclone with guide vanes inside eccentric vortex finder has a tendency to be higher. The velocity in the inner vortex has a decline except in the

center of cyclone, because of the upward main stream in the center. Such velocity distribution indicates the enhancement of the outer vortex and the weakening of the inner vortex, which is of great benefit for particle removal.

5. Conclusion

The flow field of a cyclone with guide vanes inside eccentric vortex finder is studied in this paper with Computational Fluid Dynamics Simulation. The following conclusions can be stated:

(1) Compared with the conventional cyclone, the separation efficiency of a cyclone with guide vanes inside the eccentric vortex finder increases by 7%.

(2) Compared with the conventional cyclone, the pressure drop of a cyclone with guide vanes inside the eccentric vortex finder increases no more than 12.5%.

(3) After installing guide vanes inside the vortex finder, the velocity in the inner vortex of cyclone will decrease, while that in the outer vortex tends to be higher, which is of great help for particle separation.

NOTATION

e	eccentric ratio	Z	blade number
β	hub inlet installing angle	k	middle coefficient of hub installing angle
$\triangle\beta$	shroud inlet installing angle increment	ρ	density, kg/m^3
μ_{eff}	molecular viscosity, Pa·s	G_k	turbulent kinetic energy volume production rates,
v_0	velocity, m/s	Y_d	the mass fraction of particles with a diameter larger than d
$\overline{d}$	meso-position diameter, 5 μm	n	dispersion index, 0.07

REFERENCES

S. Bernardo, A. P. Peres, M. Mori. 2005. Computational study of cyclone flow fluid dynamics using a different inlet section angle. Thermal Engineering 4(1), 18-23.

Fuping Qian, Mingyao Zhang. 2007. Effects of the Inlet Section Angle on the Flow Field of a Cyclone. Chemical Engineering Technology 30(11), 1564-1570.

Fuping Qian, Yanpeng Wu. 2009. Effects of the inlet section angle on the separation performance of a cyclone. Chemical Engineering Research and Design 87 (12), 1567-1572.

Raoufi A, Shams M, Farzaneh M, et al. 2008. Numerical simulation and optimization of fluid flow in cyclone vortex finder. Chemical Engineering and Processing 47, 128～137.

Zenz J A. 1993. Effect of Design and Operating Parameters on Cyclone Performance for CFB Boilers. Proceeding of 4th International Conference on CFB. USA, Pennsylvania.

Kirch R. Der Einfluβder Turbulenz auf die partikelbewe-gung im gaszyklon. 1982. Technical University Karlsruhe, Germany.

Hoffmann A C, Jonge R De, Arends H, et al. 1995. Evidence of the natural vortex length and its effect on the separation efficiency of gas cyclones. Filtration & Separation 32(8), 799-804.

Hoffmann AC, Arends H and Sie H. 1991. An experimental investigation elucidating the effect of solid loading on cyclone performance. Filtration and Separation 28, 188-193.